

**ANALYSIS OF THERMO-MECHANICAL
PHENOMENA AND HEAT TRANSFER
CHARACTERIZATION IN CONTINUOUS
CASTING**

PEDDURI JAYAKRISHNA



DEPARTMENT OF MECHANICAL ENGINEERING

INDIAN INSTITUTE OF TECHNOLOGY DELHI

OCTOBER 2022

**© INDIAN INSTITUTE OF TECHNOLOGY DELHI (IITD), NEW DELHI, 2022
ALL RIGHTS RESERVED**

**ANALYSIS OF THERMO-MECHANICAL
PHENOMENA AND HEAT TRANSFER
CHARACTERIZATION IN CONTINUOUS
CASTING**

by

PEDDURI JAYAKRISHNA

Department of Mechanical Engineering

Submitted

In fulfilment of the requirements of the degree of Doctor of Philosophy
to the



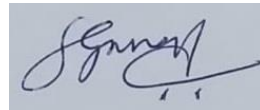
INDIAN INSTITUTE OF TECHNOLOGY DELHI

OCTOBER 2022

CERTIFICATE

I am satisfied that the thesis entitled “**ANALYSIS OF THERMO-MECHANICAL PHENOMENA AND HEAT TRANSFER CHARACTERIZATION IN CONTINUOUS CASTING**” presented by **Mr. PEDDURI JAYAKRISHNA** is worthy of the consideration for the award of the degree of **DOCTOR OF PHILOSOPHY** and is a record of the original bonafide research work carried out by him under my guidance and supervision, and the results contained in it have not been submitted in part or full to any other university or institute for the award of any degree/diploma.

I certify that he has pursued the prescribed course of research.



Dr. Prabal Talukdar

Dr. Suvankar Ganguly

Professor

Principal Scientist

Department of Mechanical Engineering

Research and Development

Indian Institute of Technology Delhi

Tata Steel, Jamshedpur

New Delhi, India

Jharkhand, India

Date:

Date:

ACKNOWLEDGMENTS

I take this occasion to show my gratitude from the bottom of my heart to my supervisors, **Prof. Prabal Talukdar** and **Dr. Suvankar Ganguly**. I am very thankful to you for giving me sufficient time for learning software, understanding the concepts and opportunities to work in a team with my senior researcher scholars. Your positive attitude, supportive nature and guidance helped me to gain sufficient motivation to finish my research.

I am always thankful to professors, Prof. Amit Gupta, Prof. M. R. Ravi, Prof. Arjun Sharma, and Prof. K. A. Subramanian, who taught me several courses at IIT Delhi and helped me in understanding the concepts and clarifying doubts during course work. I always have special gratitude towards, Prof. Sanjeev Jain, with whom I did teaching assistance for the course of Heat and Mass Transfer. I was inspired a lot by your seriousness and dedication to teaching.

I sincerely thank my senior, Dr. Saurav Chakraborty. You made me understand my mistakes while learning concepts and writing articles. I cannot describe your efforts in words and by simply saying thanks. Your inputs are always valuable to me. My research work is incomplete without incorporating your suggestions, modifications, and guidance. All my publications are an outcome of your support and encouragement. I am thankful to my senior, Dr. Ananda Srinivasa Vaka, Deputy Manager at NTPC. You have invested a great amount of your time and energy to get a better output in the field of thin slab continuous casting. I sincerely thank you for your commitment to this work. I am thankful to my senior researchers Dr. Vipul Patel, Dr. Punit Singh, Mr. Abhishek Sit, and my lab mates Mrs. Bhavna, Ms. Sonika Sharma, Mr. Mohammad Tabish Siddiqui and other friends for your kind support and cooperation.

This section is incomplete without saying special thanks to my fellow researchers, Mr. Nandyala Mahesh and Dr. Ananda Srinivasa Vaka. Our mother tongue and like-mindedness brought us together. The quality time spent with you while doing dinners is always memorable. The laughter, joy and fun sessions of ours made me forget my struggles and gave me relief from stress.

I am feeling blessed to have wonderful parents and lucky to be a younger brother to my elder brother, Mr. Vamshi Krishna. I may not be here without the strong desire of my parents to lead a purposeful life. Thanks for being with me in my life.

Above all, I am most thankful for my almighty, close to heart, dearest of all, Lord Sri Krishna, for your blessings and guidance in my life. I am relieved from all my pain and suffering in your grace. Words cannot describe my devotion to you. Thanks for providing the light in the darkness and consoling my heart.

PEDDURI JAYAKRISHNA

ABSTRACT

Producing good quality steel at higher production rates is the objective of every steel industry. Continuous casting has been the most widely used process of producing steel products from molten steel in various basic shapes which undergo subsequent operations to reach final shapes. The successful implementation of the continuous casting process in the latter half of the 19th century has seen numerous developments in casting technology, model developments, and its application for producing a wide range of end products. The thin slab continuous casting process is the most widely implemented Near net shape casting process and a very promising sustainable technology due to the use of lesser finishing operations and economic viability. The thin slab continuous casting process involves very high casting speeds to produce the castings with a smaller thickness, which results in higher productivity with less cost. To obtain high productivity, this process experiences severe drawbacks such as meniscus instability, free surface fluctuations, mould flux entrapment, etc. which are more acute as compared to the conventional continuous slab casting.

The continuous casting process is a solidification process in which liquid metal undergoes solidification and converts into liquid. The initial solidification of the liquid metal takes place in the mould. During the solidification process, the material undergoes a phase change process and shrinkage of the material takes place which causes the formation of a gap between mould walls and the solidifying metal which is in contact with the mould walls. Various approaches are proposed in the literature to address this gap effect by considering several assumptions. The first objective of this thesis develops a mathematical model to study the three-dimensional non-linear thermal resistance offered by the gap. The mathematical formulation is developed based on the principle of conservation of mass and shrinkage of the material. The expression for the thermal resistance majorly depends on the solidified shell thickness and effective thermal conductivity of the gaseous medium present at the mould-strand interface. A user-defined function (UDF) is formulated to determine the 3D variation of the solidified shell thickness along the mould length and the conservation of energy principle is used to determine the effective thermal conductivity of the gaseous medium present at the mould-strand interface. The three-dimensional fluid flow, heat transfer and solidification model along with the specially formulated boundary condition able to capture the non-linear thermal resistance. Heat transfer at the corner regions is automatically adjusted as per the

shrinkage of the material without any manual adjustments. The shell thickness obtained at the face centre near the mould exit is close to the industrial observations.

Prior knowledge of the conventional continuous casting process need not be useful to solve the problems of the thin slab continuous casting process (TSCC). Continuous deformation of solidified shell thickness due to funnel-shaped mould used in this process is the prime reason for this discrimination. Though the physics involved in both the process is the same, the TSCC is completely different in terms of geometry (aspect ratio of the thin slab, funnel shape mould, design of the nozzle, cooling water design), operating conditions (casting speed, water flow rates, cooling water velocity), magnetic equipment used for applying EMBr effect, type of mould lubrication, size of air gap formation, stability at the meniscus, cracks formations, etc. It can be understood from the literature that the heat flux empirical relations available for billet and slab casting processes cannot apply to the TSCC. The second objective of this thesis considers the interfacial heat flux profile which is determined based on the industrial plant data to study the turbulent flow, heat transfer and solidification of the solidifying thin slab in a funnel shape mould. High velocities and recirculation flow in the upper and lower regions of the mould lead to several issues like non-uniform heat transfer and hindrance in the growth of the solidified shell, etc. The high speed of the molten metal emanating from the submerged entry nozzle impinges on the narrow face at high speeds, causing remelting of the solidified shell and a thinner shell at the mould exit.

TSCC faces severe challenges towards quality control due to high casting speeds within a very narrow region, which is even more acute in funnel-shaped moulds having wide face transition from a curvilinear geometry to a linear geometry. The formation of complex recirculation flows inside the mould region are observed to be chaotic which create adverse effects such as remelting of the solidified shell and longitudinal surface defects. The third objective of this thesis is focused on controlling these complex turbulence flows to improve the thermal characteristics of the solidifying strand in TSCC.

Since the liquid metal used in the solidification process has electrical conductivity and magnetic permeability, generating strong electromagnetic forces inside the mould effectively alters the shape and size of the strong recirculation flow formations inside the mould. Hence, the method of applying the electromagnetic brake with the help of a vertical electromagnetic brake (V-EMBr) system is applied in TSCC which uses a funnel-shaped mould. Lorentz force due to the static electromagnetic field is a very effective solution to control the flow behaviour

within the mould. The V-EMBr significantly changes the flow near the narrow face and downward flow direction of liquid metal travelling towards the mould outlet. The dominating effects on surface velocities and temperatures are observed close to the narrow face since the location of V-EMBr is confined close to the narrow face. Improvement in the shell thickness and reduction of remelting effect are the major contributions of applying V-EMBr. From the observations of pathlines of fluid particles, velocity profiles near the meniscus region, growth of solidified shell at the face centre and corner region, etc., it is observed that the application of V-EMBr is succeeded in improving the thermal characteristics of the solidifying strand in TSCC.

The temperature of the liquid metal entering the mould is more than 1800 K. When the mould is subjected to continuous exposure to the high-temperature liquid metal for more than one week of duration, stresses and strains generate inside the mould. The response of the mould when it is subjected to thermal and mechanical interactions needs to be studied since they alter the shape of the mould. While studying the mechanical behaviour of the mould, creep effects have a significant contribution and is more than the elastic and plastic behaviour of the mould. The rigidity of the waterbox attached to the mould offers an additional constraint to the free deformation of the mould. The fourth objective of the thesis develops a 3D thermomechanical model using non-linear isotropic and kinematic plasticity models along with the creep model and calculate the distortion of the mould, residual stress and elastic-plastic-creep strains in an assembly of funnel-shaped mould and waterbox. Most of the funnel transition regions of the mould are accumulated with higher temperatures and hence, displacements and strain distributions are maximum in that region. Distortion of the narrow face is majorly affected by the mechanical boundary condition. It is observed that excluding the creep model highly overestimates the mechanical behaviour of the mould.

Keywords: Continuous casting; Computational Fluid Dynamics (CFD); Turbulence; Heat Transfer; Solidification; Interfacial thermal resistance; Jet impingement; Magnetohydrodynamics; Thermomechanical model; Elastic-plastic-creep model; Distortion.

सार

उच्च उत्पादन दरों पर अच्छी गुणवत्ता वाले स्टील का उत्पादन करना प्रत्येक इस्पात उद्योग का उद्देश्य है। निरंतर ढलाई विभिन्न मूल आकृतियों में पिघले हुए स्टील से स्टील उत्पादों के उत्पादन की सबसे व्यापक रूप से इस्तेमाल की जाने वाली प्रक्रिया रही है, जो अंतिम आकार तक पहुंचने के लिए बाद के कार्यों से गुजरती है। 19वीं सदी के उत्तरार्ध में निरंतर कास्टिंग प्रक्रिया के सफल कार्यान्वयन ने कास्टिंग प्रौद्योगिकी, मॉडल विकास और अंत उत्पादों की एक विस्तृत श्रृंखला के उत्पादन के लिए इसके अनुप्रयोग में कई विकास देखे हैं। पतली स्लैब निरंतर कास्टिंग प्रक्रिया सबसे व्यापक रूप से लागू नेट शोप कास्टिंग प्रक्रिया के पास है और कम परिष्करण संचालन और आर्थिक व्यवहार्यता के उपयोग के कारण एक बहुत ही आशाजनक टिकाऊ तकनीक है। पतली स्लैब निरंतर कास्टिंग प्रक्रिया में छोटी मोटाई के साथ कास्टिंग का उत्पादन करने के लिए बहुत अधिक कास्टिंग गति शामिल होती है, जिसके परिणामस्वरूप कम लागत के साथ उच्च उत्पादकता होती है। उच्च उत्पादकता प्राप्त करने के लिए, इस प्रक्रिया में मेनिस्कस अस्थिरता, मुक्त सतह में उतार-चढ़ाव, मोल्ड फ्लक्स फंसाने आदि जैसी गंभीर कमियां हैं, जो पारंपरिक निरंतर स्लैब कास्टिंग की तुलना में अधिक तीव्र हैं।

निरंतर ढलाई प्रक्रिया एक ठोसकरण प्रक्रिया है जिसमें तरल धातु जम जाती है और तरल में परिवर्तित हो जाती है। तरल धातु का प्रारंभिक जमना सांचे में होता है। ठोसकरण प्रक्रिया के दौरान, सामग्री एक चरण परिवर्तन प्रक्रिया से गुजरती है और सामग्री का संकोचन होता है जो मोल्ड की दीवारों और मोल्ड की दीवारों के संपर्क में आने वाली ठोस धातु के बीच एक अंतर के गठन का कारण बनता है। कई मान्यताओं पर विचार करके इस अंतर प्रभाव को दूर करने के लिए साहित्य में विभिन्न दृष्टिकोण प्रस्तावित हैं। इस थीसिस का पहला उद्देश्य अंतराल द्वारा प्रस्तावित त्रि-आयामी गैर-रैखिक थर्मल प्रतिरोध का अध्ययन करने के लिए गणितीय मॉडल विकसित करता है। द्रव्यमान के संरक्षण और सामग्री के संकोचन के सिद्धांत के आधार पर गणितीय सूत्रीकरण विकसित किया गया है। थर्मल प्रतिरोध की अभिव्यक्ति मुख्य रूप से मोल्ड-स्ट्रैंड इंटरफेस में मौजूद गैसीय माध्यम की ठोस शेल मोटाई और प्रभावी तापीय चालकता पर निर्भर करती है। मोल्ड लंबाई के साथ ठोस खोल मोटाई के 3 डी भिन्नता को निर्धारित करने के लिए एक उपयोगकर्ता-परिभाषित फ़ंक्शन (यूडीएफ) तैयार किया जाता है और ऊर्जा सिद्धांत के संरक्षण का उपयोग मोल्ड-स्ट्रैंड इंटरफेस में मौजूद गैसीय माध्यम की प्रभावी थर्मल चालकता को निर्धारित करने के लिए किया जाता है। गैर-रैखिक थर्मल प्रतिरोध को पकड़ने में सक्षम विशेष रूप से तैयार सीमा की स्थिति के साथ त्रि-आयामी द्रव प्रवाह, गर्मी हस्तांतरण और ठोसकरण मॉडल। कोने के क्षेत्रों में गर्मी हस्तांतरण स्वचालित रूप से बिना किसी मैनुअल समायोजन के सामग्री के संकोचन के

अनुसार समायोजित किया जाता है। मोल्ड से बाहर निकलने के पास फेस सेंटर पर प्राप्त शेल मोटाई औद्योगिक अवलोकन के करीब है।

पतली स्लैब सतत कास्टिंग प्रक्रिया (टीएससीसी) की समस्याओं को हल करने के लिए परंपरागत निरंतर कास्टिंग प्रक्रिया का पूर्व ज्ञान उपयोगी नहीं होना चाहिए। इस प्रक्रिया में प्रयुक्त फ़नल के आकार के सांचे के कारण ठोस खोल की मोटाई का लगातार विरूपण इस भेदभाव का प्रमुख कारण है। यद्यपि दोनों प्रक्रियाओं में शामिल भौतिकी समान है, इस प्रक्रिया ज्यामिति (पतले स्लैब का पहलू अनुपात, फ़नल आकार मोल्ड, नोजल का डिज़ाइन, ठंडा पानी डिज़ाइन), संचालन की स्थिति (कास्टिंग गति, पानी का पहलू अनुपात) के संदर्भ में पूरी तरह से अलग है। प्रवाह दर, ठंडा पानी वेग), ईएमबीआर प्रभाव लागू करने के लिए उपयोग किए जाने वाले चुंबकीय उपकरण, मोल्ड स्नेहन का प्रकार, वायु अंतराल गठन का आकार, मेनिस्कस पर स्थिरता, दरारें संरचनाएं इत्यादि। साहित्य ने यह भी पुष्टि की है कि बिलेट और स्लैब कास्टिंग प्रक्रियाओं के लिए उपलब्ध ताप प्रवाह अनुभवजन्य संबंध टीएससीसी पर लागू नहीं हो सकते हैं। इस थीसिस का दूसरा उद्देश्य इंटरफेशियल हीट फ्लक्स प्रोफाइल पर विचार करता है जो कि फ़नल आकार के सांचे में अशांत प्रवाह, गर्मी हस्तांतरण और जमने वाले पतले स्लैब के जमने का अध्ययन करने के लिए औद्योगिक संयंत्र डेटा के आधार पर निर्धारित किया जाता है। मोल्ड के ऊपरी और निचले क्षेत्रों में उच्च वेग और पुनरावर्तन प्रवाह कई मुद्दों को जन्म देता है जैसे गैर-समान गर्मी हस्तांतरण और ठोस खोल के विकास में बाधा, आदि। जलमग्न प्रवेश नोजल से निकलने वाली पिघला हुआ धातु की उच्च गति प्रभावित होती है उच्च गति पर संकीर्ण चेहरे पर, ठोस खोल के पिघलने और मोल्ड से बाहर निकलने पर एक पतला खोल का कारण बनता है।

इस प्रक्रिया को एक बहुत ही संकीर्ण क्षेत्र के भीतर उच्च कास्टिंग गति के कारण गुणवत्ता नियंत्रण के लिए गंभीर चुनौतियों का सामना करना पड़ता है, जो कि फ़नल के आकार के सांचों में और भी अधिक तीव्र होता है, जिसमें एक घुमावदार ज्यामिति से एक रैखिक ज्यामिति तक व्यापक चेहरे का संक्रमण होता है। मोल्ड क्षेत्र के अंदर जटिल रीसर्कुलेशन प्रवाह गठन को अराजक माना जाता है और वे प्रतिकूल प्रभाव पैदा कर रहे हैं जैसे कि ठोस खोल और अनुदैर्घ्य सतह दोष का रीमेल्टिंग। इस थीसिस का तीसरा उद्देश्य इस प्रक्रिया में जमने वाले स्ट्रैंड की तापीय विशेषताओं को बेहतर बनाने के लिए इन जटिल अशांति प्रवाह को नियंत्रित करने पर केंद्रित है।

चूंकि ठोसकरण प्रक्रिया में उपयोग की जाने वाली तरल धातु में विद्युत चालकता और चुंबकीय पारगम्यता होती है, मोल्ड के अंदर मजबूत विद्युत चुंबकीय बल उत्पन्न करने से मोल्ड के अंदर मजबूत रीसर्कुलेशन प्रवाह संरचनाओं के आकार और आकार को प्रभावी ढंग से बदल देता है। इसलिए, में

वर्टिकल इलेक्ट्रोमैग्नेटिक ब्रेक सिस्टम की मदद से इलेक्ट्रोमैग्नेटिक ब्रेक लगाने की विधि लागू होती है जो फ़नल के आकार के मोल्ड का उपयोग करती है। स्थिर विद्युत चुम्बकीय क्षेत्र के कारण लोरेंज़ बल मोल्ड के भीतर प्रवाह व्यवहार को नियंत्रित करने का एक बहुत प्रभावी उपाय है। इस प्रक्रिया ने मोल्ड आउटलेट की ओर यात्रा कर रहे तरल धातु के संकीर्ण चेहरे और नीचे की ओर प्रवाह दिशा के पास प्रवाह को महत्वपूर्ण रूप से बदल दिया। सतह के वेग और तापमान पर हावी प्रभाव संकीर्ण चेहरे के करीब देखा जाता है क्योंकि वी-ईएमबीआर का स्थान संकीर्ण चेहरे के करीब सीमित है। शेल मोटाई में सुधार और रीमेल्टिंग प्रभाव में कमी वी-ईएमबीआर लगाने का प्रमुख योगदान है। द्रव कणों की पथरेखाओं, मेनिस्कस क्षेत्र के पास वेग प्रोफाइल, चेहरे के केंद्र और कोने के क्षेत्र में ठोस खोल की वृद्धि आदि के अवलोकन से, यह देखा गया है कि ब्रेक सिस्टम के अनुप्रयोग को थर्मल विशेषताओं में सुधार करने में सफलता मिली है। इस प्रक्रिया में स्टैंड को मजबूत करना।

मोल्ड में प्रवेश करने वाली तरल धातु का तापमान 1800 K से अधिक होता है। जब मोल्ड को एक सप्ताह से अधिक की अवधि के लिए उच्च तापमान वाली तरल धातु के निरंतर संपर्क के अधीन किया जाता है, तो मोल्ड के अंदर तनाव और तनाव उत्पन्न होगा। जब मोल्ड थर्मल और मैकेनिकल इंटरैक्शन के अधीन होता है तो उसकी प्रतिक्रिया का अध्ययन करने की आवश्यकता होती है क्योंकि वे मोल्ड के आकार को बदल देते हैं। मोल्ड के यांत्रिक व्यवहार का अध्ययन करते समय, मोल्ड के लोचदार और प्लास्टिक व्यवहार की तुलना में रेंगने वाले प्रभावों का महत्वपूर्ण योगदान होता है। मोल्ड से जुड़े वॉटरबॉक्स की कठोरता मोल्ड के मुक्त विरूपण के लिए एक अतिरिक्त बाधा प्रदान करती है। थीसिस का चौथा उद्देश्य रेंगने वाले मॉडल के साथ गैर-रैखिक आइसोट्रोपिक और किनेमेटिक प्लास्टिसिटी मॉडल का उपयोग करके एक 3 डी थर्मोमैकेनिकल मॉडल विकसित करता है और फ़नल के आकार के मोल्ड की एक असेंबली में मोल्ड, अवशिष्ट तनाव और लोचदार-प्लास्टिक-रेंगना उपभेदों की विकृति की गणना करता है। मोल्ड के अधिकांश फ़नल संक्रमण क्षेत्र उच्च तापमान के साथ जमा होते हैं और इसलिए, उस क्षेत्र में विस्थापन और तनाव वितरण अधिकतम होते हैं। संकीर्ण चेहरे की विकृति यांत्रिक सीमा की स्थिति से प्रमुख रूप से प्रभावित होती है। यह देखा गया है कि रेंगने वाले मॉडल को छोड़कर मोल्ड के यांत्रिक व्यवहार को अत्यधिक महत्व देता है।

मुख्य शब्द: निरंतर कास्टिंग; अभिकलनात्मक जटिलता द्रव गतिकी ; अशांति; गर्मी का हस्तांतरण; जमाना; इंटरफेसियल थर्मल प्रतिरोध; जेट टक्कर; मैग्नेटोहाइड्रोडायनामिक्स; थर्मोमैकेनिकल मॉडल; लोचदार-प्लास्टिक-रेंगना मॉडल; विरूपण।

TABLE OF CONTENTS

CERTIFICATE.....	i
ACKNOWLEDGMENTS	ii
ABSTRACT.....	iv
संक्षेप	vii
LIST OF FIGURES	xiv
LIST OF TABLES	xix
NOMENCLATURES	xx
Chapter 1 INTRODUCTION	1
1.1. BILLET CONTINUOUS CASTING PROCESS	2
1.2. THIN SLAB CONTINUOUS CASTING PROCESS	4
1.2.1. Different types of thin slab continuous casting and rolling technologies	6
1.3. ORGANIZATION OF THE THESIS.....	9
Chapter 2 LITERATURE REVIEW AND RESEARCH OBJECTIVES.....	10
2.1. METHODS OF DETERMINING MOULD-STRAND INTERFACE HEAT TRANSFER	10
2.1.1. Thermal resistance networks.....	10
2.1.2. Empirical heat flux correlations.....	14
2.1.2.1. Billet casting.....	14
2.1.2.2. Thick slab casting	15
2.1.2.3. Thin slab casting	17
2.1.3. Inverse heat transfer technique	19
2.2. FLUID FLOW, HEAT TRANSFER, AND SOLIDIFICATION IN THIN SLAB CONTINUOUS CASTING	21
2.3. APPLICATION OF ELECTROMAGNETIC FORCE FOR FLOW CONTROL IN TSCC	23

2.3.1. Local EMBr	23
2.3.2. Single ruler type EMBr.....	25
2.3.3. Vertical EMBr (V-EMBr).....	27
2.3.4. Freestanding adjustable combination EMBr.....	28
2.3.5. Multi-pole EMBr	28
2.3.6. Multimode EMBr.....	29
2.4. THERMOMECHANICAL ANALYSIS IN FUNNEL SHAPED MOULD USED IN TSCC	30
2.4.1. Thermal analysis in thick slab and funnel-shaped thin slab moulds.....	30
2.4.2. Mechanical analysis in the funnel-shaped moulds used in TSCC	33
2.5. SUMMARY OF THE LITERATURE REVIEW.....	35
2.6. IDENTIFICATION OF RESEARCH GAP.....	37
2.7. OBJECTIVES OF THE PRESENT WORK.....	37
Chapter 3 NUMERICAL MODELLING.....	39
3.1. FLUID FLOW, HEAT TRANSFER AND SOLIDIFICATION MODEL.....	39
3.2. MAGNETO-HYDRODYNAMICS (MHD) MODEL	42
3.3. THERMOMECHANICAL MODEL.....	43
3.3.1. Thermal modelling in the funnel-shaped mould.....	43
3.3.2. Mechanical modelling in the funnel-shaped mould.....	45
3.3.2.1. Thermal strain model.....	46
3.3.2.2. Elastic model:	46
3.3.2.3. Plasticity model:	47
3.3.2.4. Creep model:	49
3.4. VALIDATION OF THE NUMERICAL MODELS.....	50
3.4.1. Validation of the solidification model	50
3.4.2. Validation of the magnetohydrodynamic (MHD) model.....	51

3.4.3. Validation of the thermal model in the thermomechanical model.....	52
3.4.4. Validation of the mechanical model in the thermomechanical model.....	53
3.5. GRID INDEPENDENCE STUDY	54
3.5.1. Grid Independence study carried out in billet domain.....	54
3.5.2. Grid Independence study carried out in thin slab domain	55
3.5.3. Grid Independence study carried out in funnel shaped mould	56
Chapter 4 DETERMINATION OF THE INTERFACIAL THERMAL RESISTANCE.....	57
4.1. INTRODUCTION	57
4.2. COMPUTATIONAL DETAILS	57
4.2.1. Formulation of the thermal resistance due to air gap.....	60
4.2.2. Determination of interface boundary condition.....	61
4.2.2.1. Calculation of non-linear thermal resistance due to air gap	62
4.2.2.2. Determination of effective thermal conductivity of the gaseous medium	64
4.3. RESULTS AND DISCUSSION	66
4.4. FINDINGS	74
Chapter 5 THERMAL CHARACTERISTICS OF A SOLIDIFYING THIN SLAB.....	76
5.1. INTRODUCTION	76
5.2. COMPUTATIONAL DETAILS	76
5.3. RESULTS AND DISCUSSION	82
5.4. FINDINGS	87
Chapter 6 VERTICAL ELECTROMAGNETIC BRAKE SYSTEM IN THIN SLAB CONTINUOUS CASTING	88
6.1. INTRODUCTION	88
6.2. COMPUTATIONAL DETAILS	88

6.3. RESULTS AND DISCUSSION	91
6.3.1. Effect of V-EMBr on flow characteristics inside the mould	91
6.3.2. Effect of V-EMBr on heat transfer characteristics inside the mould.....	96
6.3.3. Effect of V-EMBr on solidification characteristics inside the mould.....	99
6.4. FINDINGS	103
Chapter 7 THERMOMECHANICAL MODEL IN FUNNEL SHAPED MOULD	104
7.1. INTRODUCTION	104
7.2. COMPUTATIONAL DETAILS	104
7.3. RESULTS AND DISCUSSION	110
7.3.1. Thermal and mechanical behaviour of the mould.....	110
7.3.2. Effect of excluding the creep model	122
7.3.3. Effect of performing multiple cycles	124
7.4. FINDINGS	125
Chapter 8 CONCLUSIONS, FINAL REMARKS AND OUTLOOK.....	128
8.1. FINAL REMARKS AND CONCLUSIONS	128
8.2. FUTURE SCOPE.....	131
REFERENCES.....	132
LIST OF PUBLICATIONS	146
BRIEF BIODATA OF THE AUTHOR.....	147

LIST OF FIGURES

Fig. 1.1. Crude steel production in million tonnes from 1950 to 2020 (World Steel Association, 2020)	1
Fig. 1.2. Schematic of a billet continuous casting process	2
Fig. 1.3. Schematic of a thin slab continuous casting process in the mould region	6
Fig. 2.1. A simplified thermal resistance network containing resistance offered by mould wall, flux film and contact resistance between them [24]	11
Fig. 2.2. A detailed resistance network considering the resistance offered by oscillation marks [30].....	12
Fig. 2.3. Thermal resistance networks that represent (a) before and (b) after the onset of the air gap formation [34].	13
Fig. 2.4. Schematic of local EMBr system with 2 pairs of electromagnets	24
Fig. 2.5. Horizontal magnetic coil on a funnel shaped iron core	25
Fig. 2.6. Four flow patterns in thin slab casting that generate casting defects	29
Fig. 3.1. Validation of the solidification model	50
Fig. 3.2. Validation of the MHD model.....	51
Fig. 3.3. Geometric details of 3D slab mould considered in the work of Xie et al. [33].....	52
Fig. 3.4. Validation of the thermal model.....	53
Fig. 3.5. Validation of the mechanical model.....	54
Fig. 3.6. Grid independence study carried out in the billet domain.....	55
Fig. 3.7. Grid independence study carried out in the thin slab domain	55
Fig. 3.8. Grid independence study carried out in the funnel mould.....	56
Fig. 4.1. Schematic of billet continuous casting process	58
Fig. 4.2. (a) Meshing of the simulation domain along with the dimensions in mm (b) Boundary conditions applied on the simulation domain	60

Fig. 4.3. (a) Connectivity of a boundary and its group of adjacent cells (b) Connectivity of a face on a boundary and its adjacent cells.....	62
Fig. 4.4. Algorithm for determining the non-linear thermal resistance at the mould-strand interface.....	66
Fig. 4.5. (a) Velocity path lines at the mould centre plane (b) Liquid fraction contour at the mould centre plane.....	67
Fig. 4.6. Liquid fraction contours on planes located along the length of the mould	68
Fig. 4.7. Liquid fraction contour at mould outlet.....	69
Fig. 4.8. Solid shell thickness at face centre along the length of the mould.....	70
Fig. 4.9. Solid shell thickness at the corner region along the length of the mould.....	71
Fig. 4.10. Wall heat flux and shell thickness variation along the length of the mould at the face center.....	72
Fig. 4.11. Thermal resistance profiles along the length of the mould on the billet surface.....	73
Fig. 4.12. Thermal resistance profiles along the width of the mould on the billet surface.....	74
Fig. 5.1. (a) Isometric, (b) front and (c) sectional views of the bifurcated submerged entry nozzle	77
Fig. 5.2. Meshing and boundary conditions applied on the thin slab domain used in the solidification model	77
Fig. 5.3. (a) Contour plot of heat flux on hot face (b) Line plot of heat flux profiles at different locations on hot face	79
Fig. 5.4. Velocity path lines on a plane located at the centre of the mould.....	82
Fig. 5.5. Shell thickness along the length of the mould at the narrow face centre and corner region	83
Fig. 5.6. Temperature contour on the surfaces of solidifying strand	84
Fig. 5.7. Liquid fraction contours (a) on the surfaces of the solidifying strand (b) near the corner region	85
Fig. 5.8. Liquid fraction contours on planes located at different locations of the strand	86
Fig. 5.9. Liquid fraction contours at the mould exit	87

Fig. 6.1. Schematic of Vertical Electromagnetic Brake in TSCC process	89
Fig. 6.2. Meshing and boundary conditions applied on the thin slab domain used in the MHD model.....	90
Fig. 6.3. Path-lines of liquid metal at the centre of the mould without (left) and with 0.15 T (right) magnetic field	92
Fig. 6.4. Path-lines of liquid metal at the centre of the mould with 0.15 T (left) and 0.25 T (right) magnetic field	93
Fig. 6.5. Velocity profiles on free surface at the centre of the mould without and with the application of magnetic fields.....	95
Fig. 6.6. Velocity contours at the meniscus region without and with the application of magnetic fields.....	96
Fig. 6.7. Temperature profiles on free surface at the centre of the mould without and with the application of magnetic fields.....	98
Fig. 6.8. Temperature profiles at the narrow face centre along the mould length without and with the application of magnetic fields.....	99
Fig. 6.9. Shell thickness profiles at the narrow face centre without and with the application of magnetic fields.....	100
Fig. 6.10. Shell thickness profiles at the corner region without and with the application of magnetic fields.....	100
Fig. 6.11. Liquid fraction contours at the mould exit without and with the application of magnetic fields.....	102
Fig. 6.12. Shell thickness profiles on wide face at mould exit without and with the application of magnetic fields.....	102
Fig. 7.1. (a) One-fourth geometry of funnel-shaped mould and waterbox (b) Meshing of the simulation domain.....	105
Fig. 7.2. Geometry and dimensions of funnel mould confined only to copper plate thickness	106
Fig. 7.3. Cooling channel geometry and dimensions (a) Cooling channel geometry inside the mould (b) Section at the meniscus region (c) Channel dimensions in the selected section...	106

Fig. 7.4. Geometric details and boundary conditions of the funnel-shaped mould and waterbox	108
Fig. 7.5. The algorithm of thermomechanical model.....	109
Fig. 7.6. Contour plot of temperature distribution on the meniscus and hot face of the mould	111
Fig. 7.7. Temperature profiles on the hot face of the wide faces at distinct locations in the (a) width direction (b) length direction	112
Fig. 7.8. Displacement profiles on hot face of the wide face at distinct locations in the (a) width direction (b) length direction	113
Fig. 7.9. (a) Temperature and (b) Displacement profiles on the narrow face along the mould length	114
Fig. 7.10. Comparison of temperature and displacement profiles on hot face of the mould (a) Wide face ($X = 200$ mm) (b) Narrow face ($Y = 0$).....	115
Fig. 7.11. Distortion of the wide face (a) towards and away from the liquid metal (100 times scaled in Y-direction) (b) along mould top and bottom (100 times scaled in Z-direction) ...	116
Fig. 7.12. Distortion of wide face towards and away from the symmetric face ($X = 0$) (100 times scaled in X-direction)	117
Fig. 7.13. Distortion of the narrow face towards and away from the liquid metal (100 times scaled in X-direction).....	118
Fig. 7.14. Displacement profiles along the mould length on hot face of the wide plate at the end of cooling and heating (casting) operations	119
Fig. 7.15. (a) Thermal strain and (b) von Mises stress distribution on the hot face of the mould	120
Fig. 7.16. von Mises stress distribution on (a) mould and waterbox (b) cooling channels ...	121
Fig. 7.17. Equivalent strain distribution on the hot faces of the mould (a) Plastic strain (b) Creep strain.....	122
Fig. 7.18. Comparison of displacement fields between elastic-plastic-creep and elastic-plastic models on hot face of the mould (a) Wide face ($X = 200$ mm) (b) Narrow face ($Y = 0$).....	123

Fig. 7.19. Comparison of equivalent plastic strain distribution with (a) elastic-plastic-creep and (b) elastic-plastic models 123

Fig. 7.20. Effect of performing multiple cycles on displacement fields on hot face of the mould (a) Narrow face ($Y = 0$) (b) Narrow face ($Y = 35$ mm) (c) Wide face ($X = 0$) (d) Wide face ($X = 200$ mm)..... 125

LIST OF TABLES

Table 1.1. List of some plants with Compact Strip Production (CSP) technology	7
Table 1.2. List of plants with various thin slab casting technologies	8
Table 2.1. Interface heat flux correlations proposed for billet casting	15
Table 2.2. Interface heat flux correlations proposed for thick slab casting	16
Table 2.3. Interface heat flux correlations proposed for thin slab casting	17
Table 2.4. Casting conditions and results obtained in funnel-shaped moulds used in TSCC..	32
Table 3.1. Model parameters as a function of temperature for the plasticity model	48
Table 3.2. Model parameters for the creep model	49
Table 3.3. Data for the validation of the solidification model	50
Table 3.4. Data for the validation of the MHD model	52
Table 3.5. Data for the validation of the mechanical model	54
Table 4.1. Geometric details, operating conditions, and thermophysical properties of 0.22%C (wt%) steel	65
Table 4.2. Piece-wise linear function of Thermal conductivity (K)	65
Table 4.3. Piece-wise linear function of Specific heat (C_p)	65
Table 5.1. Thermal properties of 0.065%C (wt%) steel	80
Table 5.2. Chemical composition of steel in weight percentages (wt%)	80
Table 5.3. Piece-wise linear function of density (ρ)	81
Table 5.4. Casting conditions and simulation parameters considered in the simulations.....	81
Table 6.1. Electromagnetic properties of steel.....	89
Table 7.1. Thermomechanical properties and operating conditions of copper mould.....	107
Table 7.2. Thermomechanical properties of steel waterbox	107

NOMENCLATURES

Symbols	Description	Unit
A	Creep rate coefficient	1/s
A_{mush}	Mushy zone parameter	kg/m ³ .s
\vec{B}	Magnetic field or total magnetic field	T
\vec{B}_0	Externally imposed magnetic field	T
\vec{b}	Induced magnetic field due to fluid motion	T
\mathbf{C}	Elasticity tensor	N/m ²
C_μ	Function in definition of turbulent viscosity	-
C_1, C_2	Model parameters in turbulence equations	-
C_k	Kinematic hardening modulus	Pa
C_p	Specific heat	J/kg. K
D	Diameter	m
E	Young's modulus of elasticity	Pa
\mathbf{F}	Deformation gradient tensor	-
\vec{F}_{ES}	Solidification source term in the energy equation	kg/m. s ⁴
\vec{F}_L	Lorentz force	N
\vec{F}_{MS}	Solidification source term in the momentum equation	kg/m ² . s ²
f	Body force	N
f_l	Liquid fraction	-
G_k, G_b	Generation of the turbulence kinetic energy due to mean velocity gradients and buoyancy respectively	kg/m. s ³
\vec{g}	Acceleration due to gravity	m/s ²
H	Total enthalpy	J/kg
h	Convective heat transfer coefficient	W/m ² K
h_a	Convective heat transfer coefficient of the medium at meniscus	W/m ² K
h_{sen}	Sensible enthalpy	J/kg
h_w	Cooling water heat transfer coefficient	W/m ² K
h_m	Convective heat transfer coefficient in the mould	W/m ² K

h_{net}	Net heat transfer coefficient	W/m ² K
I	Identity matrix	-
\vec{j}	Induced current density	A/m ²
K	Thermal conductivity	W/m.K
K_w	Thermal conductivity of water	W/m.K
K_{cu}	Thermal conductivity of copper alloy of mould	W/m.K
K_{eff}	Effective thermal conductivity of gaseous medium	W/m.K
K_{tot}	Effective thermal conductivity in turbulent flow	W/m.K
k	Turbulent kinetic energy	m ² /s ²
L	Latent enthalpy	J/kg
L_{mould}	Length of the mould	m
m	Time hardening exponent	-
n	Stress hardening exponent	-
Pr_t	Turbulent Prandtl number	-
p	Pressure	Pa
q_{avg}	Average heat flux from the mould	W/m ²
Q	Creep activation energy	J/mol
\vec{Q}''	Heat flux	W/m ²
Q_{pl}	Plastic potential	Pa
R	Universal molar constant	N.m/K
Re	Reynolds number	-
R_{cu}	Thermal resistance due to copper mould thickness	m ² . K/W
R_{flux}	Thermal resistance due to mould flux film	m ² . K/W
R_{gap}	Thermal resistance due to gap	m ² . K/W
$R_{interface}$	Interfacial thermal resistance	m ² . K/W
$R_{solid,flux}$	Thermal resistance due to solid flux	m ² . K/W
$R_{solid,cond}$	Conduction resistance offered by solid flux	m ² . K/W
$R_{solid,rad}$	Radiation resistance offered by solid flux	m ² . K/W
$R_{liquid,flux}$	Thermal resistance due to liquid flux	m ² . K/W
$R_{liquid,cond}$	Conduction resistance offered by liquid flux	m ² . K/W
$R_{liquid,rad}$	Radiation resistance offered by liquid flux	m ² . K/W

R_{air}	Thermal resistance due to air gap	$m^2 \cdot K/W$
$R_{air,cond}$	Conduction resistance offered by air gap	$m^2 \cdot K/W$
$R_{air,rad}$	Radiation resistance offered by air gap	$m^2 \cdot K/W$
R_{rad}	Thermal resistance due to radiation heat transfer	$m^2 \cdot K/W$
R_{mould}	Resistance offered by mould wall	$m^2 \cdot K/W$
R_{total}	Total thermal resistance between strand and cooling water	$m^2 \cdot K/W$
R_w	Thermal resistance due to cooling water	$m^2 \cdot K/W$
R_{nozzle}	Radius of submerged entry nozzle at inlet	m
S_k	Source term in the turbulent kinetic energy equation	$kg/m \cdot s^3$
S_ε	Source term in the turbulent dissipation rate equation	$kg/m \cdot s^4$
T	Temperature	K
T_a	Temperature of the surrounding above meniscus	K
T_{break}	Break point temperature of the mould powder	$^\circ C$
T_{ref}	Reference temperature for thermal expansion	K
T_∞	Free stream temperature	K
T_L	Liquidus temperatures	K
T_S	Solidus temperatures	K
T_M	Temperature of mould on hot face side	K
T_P	Temperature of solid flux film	K
T_{surf}	Surface temperature of the solidified shell	K
T_{flow}	Melting temperature of the mould powder	$^\circ C$
T_{fsol}	Mould slag solidification temperature	K
T'_S	Steel shell surface temperature at oscillation mark root	K
T_{sol}	Solidus temperature of 0.044%C steel	K
T_{cry}	Temperature of mould flux crystallization	K
T_A	Interface temperature at the air gap side	K
T_B	Interface temperature at the solid flux side	K
T_w	Average temperature of cooling water taken at inlet and outlet	K
ΔT	Degree of superheat	K
t	Time	s

τ_{cu}	Thickness of copper mould	m
t_{ref}	Reference time	s
t_{shift}	Time shift parameter	s
\vec{u}	Displacement vector	m
\vec{V}	Mean flow velocity vector	m/s
V_c	Casting velocity	m/s
\dot{V}_w	Volume flow rate of water	m ³ /s
x_l	Liquid steel thickness	m
x_s	Solidified shell thickness	m
\vec{X}	Material coordinate vector	-
$\vec{x}(\vec{X}, t)$	Spatial coordinate vector	m
x, y, z	Spatial coordinates in rectangular coordinate system	-
X, Y, Z	Material coordinates in rectangular coordinate system	-
Y	Yield function	Pa

Greek letters

Symbols	Description	Unit
α	Coefficient of thermal expansion	1/K
$\alpha_k, \alpha_\varepsilon$	Inverse effective Prandtl numbers in turbulence	-
β	Saturation exponents	-
ε	Turbulent dissipation rate	m ² /s ³
λ	Plastic multiplier	-
μ	Dynamic Viscosity	kg/m.s
μ'	Magnetic permeability	H/m
ν	Poisson's ratio	-
ρ	Density	kg/m ³
σ'	Electrical conductivity	siemens/m
σ	Cauchy stress tensor	Pa
σ_b	Back-stress	Pa
σ_{ref}	Reference stress	Pa

σ_{mises}	von Mises equivalent stress	Pa
σ_{sat}	Saturation flow stress	Pa
σ_{ys}	Yield stress	Pa
σ_{ys0}	Initial yield stress	Pa
$\phi(\sigma)$	Equivalent stress	Pa
φ	Variable containing small value	-
∂	Partial differential operator	-
ϵ	External emissivity	-
∇	Gradient operator	1/m
ϵ_{pe}	Effective plastic strain	-
$\dot{\epsilon}_{pe}$	Equivalent plastic strain rate	-
ϵ_{pl}	Plastic strain tensor	-
γ_k	Kinematic hardening parameter	-

Subscripts

cr	Creep
el	Elastic
eff	Effective value
h	Hydraulic
lam	Laminar
mises	von Mises
pl	Plastic
ref	Reference value
sen	Sensible
slag	Mould slag
tot	Total
th	Thermal
tur	Turbulent
w	Cooling water